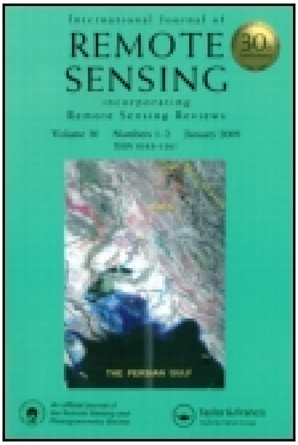

International Journal of Remote Sensing
Publication details, including instructions for authors and subscription information:
http://www.tandfonline.com/loi/tres20

Water quality remote sensing in the visible spectrum

K. Ya. Kondratyev, D. V. Pozdnyakov & L. H. Pettersson

Available online: 25 Nov 2010

INT. J. REMOTE SENSING, 1998, VOL. 19, NO. 5, 957–979

Water quality remote sensing in the visible spectrum

K. YA. KONDRATYEV,† D. V. POZDNYAKOV‡ and
L. H. PETTERSSON§

† Scientific Research Center for Ecological Safety, Korpousnaya str., 18, 197042 St. Petersburg, Russia
‡ Nansen International Environmental and Remote Sensing Center, Korpousnaya str., 18, 197042 St. Petersburg, Russia
§ Nansen Environmental and Remote Sensing Centre, Edv. Griegsv., 3A, N-5037, Solheimsviken/Bergen, Norway

(*Received 14 November 1995; in final form 2 July 1997*)

Abstract. The development of water quality retrieval algorithms is discussed in terms of causal dependence of the upwelling spectral radiance upon the water composition. Unlike clear marine/oceanic waters, for which linear regression retrieval relationships are valid, inland and coastal zone water masses with a high degree of optical complexity necessitate the development of more subtle retrieval approaches. At the basis of such approaches are models considering the conjoint optical impact of several co-existing aquatic components on the water leaving radiance spectral distribution. Such a model for Lake Ladoga is described. Monte Carlo simulations have been performed to analyse the spectral and angular variations of the upwelling radiance scattered by the water column into the atmosphere. Optimal conditions for conducting water quality remote sensing in case of natural waters of various optical complexity are explored and relevant recommendations are formulated.

1. Introduction

The urgency of the water quality problem mostly resides in a continuous deterioration of ecological status of inland water basins, coastal zones of seas and oceanic gulfs (NASA 1986, Petrova 1995). This is largely due to an unprecedented intensification of natural eutrophication processes going on in the water bodies either encapsulated by a single continent or constituting marine/oceanic marginal areas. Their natural 'ageing' is immensely accelerated because of extensive anthropogenic inputs of nutrients (phosphorous and nitrogen chemical compounds, in the first place) in the aquatic environments. Often, the eutrophication is additionally stimulated by water temperature increase, due to thermal industrial inflows and/or anthropogenic basin shallowing (as a result of enhanced run-off and river drift input). A substantial increase in water turbidity, caused by human-induced heightening of concentrations of suspended and dissolved matter, is also capable of contributing to the water temperature rise. These factors lead to a rapid transition of the basin to a higher trophic level which, in turn, entails algal bloom events, anoxia, and eventually, a dramatic deterioration of water quality parameters (Henderson-Sellers and Markland 1987).

The outlined causal chain does not cease at this step. The primary production growth in such water bodies reflects on carbon and sulphur cycles thus influencing atmospheric processes directly related to local and global climate changes (Kondratyev 1992).

The pioneer investigations on the applicability of remote sensing in the visible spectrum to studying water quality related problems go back to the 1960s and 1970s, and were mainly meant to determine algae chlorophyll concentrations in clear and optically simple marine and oceanic waters, i.e., waters assigned, according to the Morel classification (Morel and Prieur 1977) to case I waters.

Our present study is focused on the examination of remote sensing technique feasibilities in case of monitoring *inland* waters which, along with marine coastal waters, basically do not belong to case I waters, and are usually referred to as non-case I waters (Bukata *et al.* 1995). These waters present serious difficulties for successful application of remote sensing techniques because of their complex optical properties. A number of researchers have conducted studies in this area (Bukata *et al.* 1981, 1983, Kirk 1983, 1984, Melack 1983, Guittelson *et al.* 1986, Fisher *et al.* 1991, Dekker *et al.* 1995). However, the remotely sensing of turbid non-case I waters still presents many problems residing, first, in poor separability of signals stemming from different constituents of such waters.

To investigate these problems, the following sequence of research seems appropriate. First, we analyse, by means of numerical modelling, the sensitivity of the radiance signal captured by a remote sensor to variations of both the major optically-active components (OAC) abundant in the water column, and the geometry of the water surface illumination by the sun and viewing by the remote sensor. These analyses are liable to reveal optimal conditions conducting practical remote sensing of natural water bodies. Second, we examine the retrieval methodology physical background and operational water quality retrieval techniques applicable to hydro-optical situations which could be encountered in waters ranging from clear oceanic to turbid inland/marine coastal zone (i.e., case I and non-case I) waters.

The efficiency of traditional regression (parametric) algorithms in the form of parametrizations based on constant coefficients established from statistical data on relations between water leaving radiance at two or more wavelengths, and the corresponding phytoplankton chlorophyll or suspended matter concentrations, are to be compared with the appropriateness and robustness of more subtle algorithms. The latter, as opposed to regression algorithms, are not based on statistical parametrizations, but on more sophisticated procedures, such as multivariate optimization techniques (Bukata *et al.* 1985, Kondratyev *et al.* 1990), maximum likelihood (Doubovik *et al.* 1994, Tanis and Pozdnyakov 1995), neural networks (Schiller and Doerffer 1997) and others. In this work we shall focus on the multivariate optimization techniques.

In view of the common use in remote sensing of *water colour* as a parameter characterizing the ecological state of the World Ocean (NASA 1986, Hooker and Esaias 1993), we place a special emphasis on the assessment (through numerical modelling) of realistic potentials of this parameter.

Following the research outline specified above, the numerical simulations performed in this study, as well as retrievals of water quality parameters in Lake Ladoga, were based both on the Lake Ladoga waters optical model developed earlier by Kondratyev *et al.* (1990) (see also Bukata *et al.* 1991, 1995), and on ship-borne remote and *in situ* data concurrently collected in Lake Ladoga.

2. Numerical simulation approaches

2.1. *Monte Carlo simulations*

Numerical experiments have been carried out using the Monte Carlo (M-C) technique described elsewhere (Kondratyev *et al.* 1987). When running the M-C simulations, the following processes were taken into account: photon interactions with wind-roughened water surface, absorption, and elastic scattering of light on molecules of atmospheric gases and on aerosols, as well as on water molecules and on hydrosols. Simulations were performed by way of designing a homogeneous Markov chain of photon collisions and employing a local estimation technique (Kargin 1983). A cloudless atmosphere was designed using the scattering and absorption coefficients suggested by McClatchey *et al.* (1982). Models of rural, tropospheric, and background stratospheric aerosols were related, respectively, to layers 0–2, 2–10, and 10–30 km. The vertically integrated optical depth of such an atmosphere proved to be 0·8, 0·5, 0·48, 0·45, 0·39, and 0·29 at wavelengths 400, 500, 520, 550, 600, and 800 nm respectively. The optical depths of the first (starting from the earth surface) 10 km-atmospheric layer at $\lambda = 400$, 600, and 800 nm were 0·201, 0·129, and 0·102, respectively.

For the atmospheric layers specified above, the aerosol phase functions were calculated with Mie formulae using the aerosol size distributions given in McClatchey *et al.* (1982). The estimates of refraction indices for aerosol particles as well as the limits of variations of both particle sizes and their refraction indices were also taken from McClatchey *et al.* (1982).

The water basin was assumed to be 60 m deep. It was also assumed that its hydro-optical properties are determined by pure water, phytoplankton (chl), suspended minerals (sm) and dissolved organic carbon (doc). The phytoplankton, denoted as chl, nevertheless, represent a community of chlorophyll bearing algae cells which are assumed to both absorb and scatter the incident light. It is further assumed that suspended mineral particles are also absorbers and scatters of light, whereas the doc molecules are considered exclusively as absorbers, on the basis that their scattering contribution is, first, indistinguishable from that of pure water, and, second, insignificant in comparison with water's (Fadeev and Churbanov 1981). The water column was subdivided into several layers characterized by certain vertical profiles of chl concentrations, whereas sm and doc concentrations were assumed vertically invariable. Spectral absorption and scattering coefficients of H_2O and absorption and backscattering cross sections, chl, sm, and doc constituting the Lake Ladoga waters optical model (see below) were used in our calculations. The model does not account for the optical impact of detritus because of the lack of appropriate data collected in our field experiments. The hydrosol phase functions were obtained using Mie formulae, and the particle size distribution parametrization derived as the best fit to the available experimental data on Lake Ladoga (Kondratyev *et al.* 1987):

$$f(r) = 3{\cdot}09 \times 10^{8} r^{-3{\cdot}575} \tag{1}$$

where $0{\cdot}001 < r < 2$ nm.

The optical depth of the modelled water basin, depending on concentrations of chl, sm and doc typical of Lake Ladoga, lay within $180 < t_{400\,\mathrm{nm}} < 630$, $36 < t_{600\,\mathrm{nm}} < 486$, $30 < t_{800\,\mathrm{nm}} < 360$. The bottom albedo was assumed to be zero. The water-atmosphere interface was designed as an array of elementary facets whose normals were distributed following a 'truncated' Cox-Munk parametrization with the exponential part set to unity. Therefore, the elevations of facets in the model were taken as zero. The effect of foam formations was not included in our model.

2.2. *Water colour simulations*

The human eye senses the water colour through capturing and analysing the radiance signal coming up from the water surface. Actually, this signal consists of two components originating from the light both reflected by the water surface and scattered by the water column back into the atmosphere. It is the second component which carries the information about the colorimetric properties of the water column, and consequently, about the OAC concentrations.

The relationship between the radiance coming up from beneath the water surface, i.e., the above surface radiance $L_u(+0)$ and the inherent hydrooptical characteristics (coefficients of absorption a and backscattering b_b) could be parametrized via the volume reflectance parameter R (Austin 1974, Bukata *et al.* 1981):

$$L_u(+0) = R[1 - \rho(\theta)]E_d(-0)/\pi n^2(1 - 0{\cdot}48R) \quad (2)$$

where $\rho(\theta)$ is the Fresnel reflectivity within the field of view of the remote sensor at the nadir angle of viewing (θ), n is the relative index of refraction of water to air, and $R = E_u(-0)/E_d(-0)$, $E_u(-0)$, $E_d(-0)$ are the upwelling and downwelling subsurface irradiances respectively.

To relate the volume reflectance R to the coefficients a and b_b, a number of parametrizations have been suggested, of which for the conditions of water bodies with a wide range of variations in water turbidity, the most adequate equation is the one developed by Jerome *et al.* (1988):

$$\begin{aligned} R &= (1/\mu_0)0{\cdot}319 b_b/a \quad 0 < b_b/a < 0{\cdot}25 \\ R &= (1/\mu_0)[0{\cdot}267 b_b/a + 0{\cdot}013] \quad 0{\cdot}25 < b_b/a < 0{\cdot}5 \end{aligned} \quad (3)$$

where $\mu_0 = \cos(\theta_0)$, θ_0, being the in-water solar refracted angle; $\mu_0 = 0{\cdot}858$ for overcast conditions. This relation is strictly applicable for high solar elevations, and at large solar zenith angles, a certain correction term is reportedly required (Bukata *et al.* 1995).

The inherent hydro-optical characteristics are known to be additive in nature, i.e.,

$$\begin{aligned} a &= a_w + \sum_i a_i \\ b_b &= (b_b)_w + \sum_i (b_b)_i \end{aligned} \quad (4)$$

where subscripts w and i refer respectively to water molecules and OAC.

If the OAC number is limited by three (i.e., by chl, sm and doc) and the cross sections a^* and b_b^* (i.e., absorption and backscattering coefficients divided by the respective optically active component concentration) are employed, then equation (4) could be rewritten as:

$$\begin{aligned} a &= a_w + C_1 a_1^* + C_2 a_2^* + C_3 a_3^* \\ b_b &= (b_b)_w + C_1 (b_b)_1^* + C_2 (b_b)_2^* + C_3 (b_b)_3^* \end{aligned} \quad (5)$$

where $i = 1 \ldots 3$ are chl, sm and doc respectively, and C_i is the concentration of a naturally occurring OAC.

Once the cross sections are known, and the spectral values of $E_d(-0)$ are either directly measured *in situ* or calculated from a known optical model of the atmosphere, the water leaving radiance $L_u(+0)$ could be found and further used for assessing the tristimulus values given by

$$X' = \int x''(\lambda) L_u(+0, \lambda)\, d\lambda$$

$$Y' = \int y''(\lambda) L_u(+0, \lambda)\, d\lambda \qquad (6)$$

$$Z' = \int z''(\lambda) L_u(+0, \lambda)\, d\lambda$$

where x'', y'', z'' are the Comité International d'Eclairage (1957) colour mixtures (for red, green, and blue respectively) for equal energy spectra, obtained from CIE tables.

The chromaticity co-ordinates could then be obtained from the equations:

$$x = X'/(X' + Y' + Z')$$

$$y = Y'/(X' + Y' + Z') \qquad (7)$$

$$z = Z'/(X' + Y' + Z')$$

So far as $x + y + z = 1$, two chromaticity co-ordinates adequately represent colour in a chromaticity diagram, and the chromaticities can be displayed as two-dimensional plots of either y (green)–z (blue), or x (red)–y (green).

Using the CIE colour values, $x''(\lambda)$, $y''(\lambda)$, $z''(\lambda)$, and assuming monochromatic light of a given wavelength as the spectrum $E(\lambda)$, the CIE chromaticity co-ordinates may be obtained for that particular wavelength. By repeating this procedure, CIE chromaticity co-ordinates may be obtained for each wavelength throughout the visible spectrum. All the (x, y) pairs obtained in such a manner are plotted in figure 1. For a white spectrum (i.e., $L(\lambda) = \text{constant}$) $x = y = z = 0{\cdot}333$. This defines the achromatic colour or white point **S** illustrated in figure 1. A numerical value of colour is then obtained by drawing a line from this white point **S** through the plotted chromaticity values of the measured spectrum (as indicated by point **Q**). The intersection of the line **S**–**Q** with the curve envelope of figure 1 (indicated by point **A**)

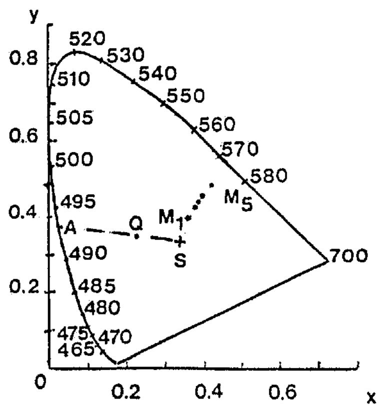

Figure 1. The Y (green) and X (red) chromaticity co-ordinates appropriate for each wavelength throughout the visible spectrum. The white point S is shown for $Y = X = 0{\cdot}333$. The points Q and A are explained in the text, as are the points M_1 to M_5 representing combinations of Lake Ladoga OAC. Numbers (400–700) are wavelengths in nm.

specifies the dominant wavelength λ_{dom} that will be herein considered as the colorimetric definition of the natural water body.

In our numerical simulations of water colour, the OAC cross sections were taken from the Lake Ladoga waters optical model reported by Kondratyev *et al.* (1990). Values of $E_d(-0, \lambda)$, $E_u(-0, \lambda)$ and $R(-0, \lambda)$ as measured *in situ* from a scientific vessel under clear skies and calm conditions in Lake Ladoga (Kondratyev *et al.* 1990) were employed to further determine the water colour characteristics specified above. The x'', y'', z'' values were taken from Yerlov (1976).

3. The Lake Ladoga waters optical model

Lake Ladoga is the largest natural inland water body in Europe. Formed some 12 000 years ago and measuring 220 km × 83 km with the water surface of about 17 800 km^2, Lake Ladoga encapsulates almost 1000 km^3 of fresh water. Extending from north to south by more than 1000 km and from west to east by about 600 km, the lake watershed is about 260 000 km^2. The bottom topography is uneven: its average and maximum depths are 51 and 230 m respectively. The northern part of the lake is deep (150–200 m), and the coastline is jagged by a wealth of long and narrow fjords. The depths in the southern part are much smaller and progressively diminish southwards. The southern coastline is formed by a number of large open bays, with depths to less than 5–10 m. The geographical position (59°–61°N), as well as the morphometric characteristics of Lake Ladoga, predetermined its strictly oligotrophic status from the moment of the lake formation. This status persisted until the early 1960s. Intense industrialization and extensive agricultural development have resulted in dramatic changes to the lake ecology. Although remaining a deep, large, and rather cold water body, Lake Ladoga has developed in previous decades a stable mesotrophy with extensive seasonal blooming events (Petrova 1995). The algae chlorophyll concentrations during these periods may reach values up to 15–20 μg l^{-1} and even higher in the coastal zone. The average DOC concentrations are about 8·0 mgC l^{-1}, although, in some coastal areas the DOC content can be as large as 10 mgC l^{-1}. The concentrations of suspended minerals vary from about 0·1–6–8 mg l^{-1}, with the mean annual values ranging from 0·8–1·6 mg l^{-1}.

Conducted in the late 1980s, our extensive field measurements of subsurface volume reflectance spectra supplemented by a simultaneous collection of water samples in Lake Ladoga to determine the concentrations of suspended minerals, chlorophyll, and DOC resulted (through the employment of the Levenberg-Marquardt [L-M] multivariate optimization technique described below) in an establishment of absorption and backscattering cross sections of the principal OAC (Kondratyev *et al.* 1990, Bukata *et al.* 1991) (table 1). The spectral cross sections listed in table 2 constitute an optical model of the Lake Ladoga waters assuming that at any instant of time a natural water mass may be adequately defined as a homogeneous combination of pure water, suspended organic material (represented by the chl concentration), suspended inorganic material (represented by the sm concentration), and dissolved organic material (represented by the doc concentration).

Although the definitive optical model should consider the cross sections of every distinct aquatic component present in natural water masses as well as account for any temporally-varying characteristics of these components, such a model is clearly unattainable, and a sensible confinement of the present optical model to a few principal components seems quite warrantable. The reasoning for our choice of chl,

Table 1. Absorption and backscattering coefficients of water (w) and absorption and back-scattering cross-sections of phytoplankton (chl), suspended minerals (sm) and dissolved organic carbon (doc) for Lake Ladoga.

λ (nm)	a_w (m^{-1})	a^*_{chl} ($m^2 mg^{-1}$)	a^*_{sm} ($m^2 g^{-1}$)	a^*_{doc} ($m^2 (gC)^{-1}$)	$(b_b)_w$ (m^{-1})	$(b_b)^*_{chl}$ ($m^2 mg^{-1}$)	$(b_b)^*_{sm}$ ($m^2 g^{-1}$)
410	0·038 00	0·038 00	0·265 00	0·280 00	0·002 29	0·0012 40	0·023 00
430	0·026 00	0·040 00	0·230 00	0·250 00	0·001 86	0·0012 30	0·025 00
450	0·017 00	0·041 00	0·200 00	0·230 00	0·001 52	0·0012 10	0·027 00
470	0·017 00	0·040 00	0·180 00	0·180 00	0·001 28	0·0012 00	0·029 00
490	0·021 00	0·034 00	0·160 00	0·160 00	0·001 08	0·0012 10	0·030 50
510	0·026 00	0·028 00	0·145 00	0·140 00	0·000 91	0·0012 40	0·032 00
530	0·030 00	0·022 00	0·130 00	0·125 00	0·000 91	0·0012 70	0·033 00
550	0·037 00	0·018 00	0·120 00	0·110 00	0·000 66	0·0012 90	0·033 50
570	0·057 00	0·015 00	0·110 00	0·100 00	0·000 58	0·0012 80	0·033 00
590	0·112 00	0·013 00	0·105 00	0·090 00	0·000 50	0·0012 70	0·032 50
610	0·236 00	0·012 00	0·100 00	0·080 00	0·000 44	0·0012 70	0·032 00
630	0·274 00	0·012 00	0·100 00	0·070 00	0·000 38	0·0012 60	0·031 00
650	0·303 00	0·020 00	0·105 00	0·060 00	0·000 33	0·0012 20	0·029 00
670	0·370 00	0·025 00	0·115 00	0·050 00	0·000 30	0·0011 60	0·027 00
690	0·463 00	0·016 00	0·125 00	0·050 00	0·000 26	0·0010 80	0·025 00

Table 2. Data from *in situ* measurements of the phytoplankton chlorophyll, suspended minerals and dissolved organic carbon concentrations at stations $M_1 - M_5$ in Lake Ladoga.

Station Concentration	M_1	M_2	M_3	M_4	M_5
C_{chl} ($\mu g\, l^{-1}$)	0·5	1·5	2·7	5·6	9·0
C_{sm} ($mg\, l^{-1}$)	0·4	0·6	0·8	1·2	0·8
C_{doc} ($mgC\, l^{-1}$)	7·0	7·0	7·0	8·5	7·5

sm, and doc as principal OAC in the model has been given in full detail elsewhere (Kondratyev *et al.* 1990). Since the water mass is assumed here to be homogeneous, the current model does not include layering effects. Also, no provision is incorporated for chemical impurities. Nevertheless, the actual feasibility of the model in question depends on the relative significance of optical effects caused by the water mass properties overlooked by the model. The degree of adequacy of the optical model (which in general seems to be explicitly time and location dependent) can be assessed through extensive field retrieval experiments involving shipborne subsurface volume reflectance spectra measurements supplemented by water sampling to determine the concentrations of chl, sm, and doc for validation purposes. Applying the above-mentioned L-M technique to the measured subsurface volume reflectance spectra, and using the appropriate optical model in the form of absorption and back-scattering cross sections, it is possible to infer the desired concentration vector $\boldsymbol{C}$ $(1, C_{chl}, C_{sm}, C_{doc})$ and then to compare it with its directly (*in situ*) measured counter-part. The results of these retrieval and validation studies performed in Lake Ladoga have shown (see section 4.3) that there is a good conformity between the retrieved and actually measured values of C_{chl}, C_{sm}, and C_{doc}. Reiterated in midsummer time during three consecutive years, these retrieval and validation studies in Lake Ladoga gave invariably good results thus pointing to the fact that the elaborated optical model proves to be reasonably adequate. Its comparison with the optical model suggested for Lake Ontario by Bukata *et al.* (1981) reveals a considerable closeness in magnitudes and spectral variations of absorption and backscattering cross sections for chl, sm, and doc (Bukata *et al.* 1991). This somewhat surprising conformity comes, in all probability, from likeness in their latitudinal location, watershed specific features (including soil composition), and hydrobiota communities inherent in both lakes (Petrova 1995). Characteristic of Lake Ladoga and being alike the set of cross sections for Lake Ontario, our optical model has been further tried for the retrieval of OAC from remotely-sensed data obtained on Lake Onega—the second largest lake in Europe, located to the north-east of Lake Ladoga. In this case, as well, the retrieval results proved to be satisfactory (Kondratyev *et al.* 1990), thus suggesting that the optical model in question could be applicable, if caution is exercised, to other deep and relatively cold temperate lakes which have developed a stable mesotrophy.

4. Results of numerical modelling

4.1. *Monte Carlo simulations of spectral and angular variations of the upwelling radiance*

In discussing the results of the Monte Carlo simulations, the following notations will be employed: $L_u(+0, \lambda)$ is the spectral radiance scattered by a water column out into the atmosphere; $L_{rs}(+0, \lambda)$ is the spectral radiance upwelling from the water surface (this entity comprises $L_u(+0, \lambda)$, the Fresnel reflection component $L_{(\mathrm{fresnel})}$ and, in the general case, the radiance contribution from the intervening atmospheric layer, i.e., the path radiance $L_{(\mathrm{path})}$). The angle denominations are illustrated in figure 2. For simplicity reasons $L_u(+0, \lambda)$ and $L_{rs}(+0, \lambda)$ will be written below as $L_u(\lambda)$ and $L_{rs}(\lambda)$.

The first step of our simulations was aimed at assessing the sensitivity of $L_u(\lambda)$ and $L_{rs}(\lambda)$ to the vertical distribution of chl concentration in the water body. Several options of chl profiles have been tried (figure 3), whereas concentrations of sm and doc were kept vertically invariant. Results of numerical experiments (the computations refer to the solar spectral region $400 < \lambda < 700$ nm, solar zenith angle $\vartheta_0 = 30°$,

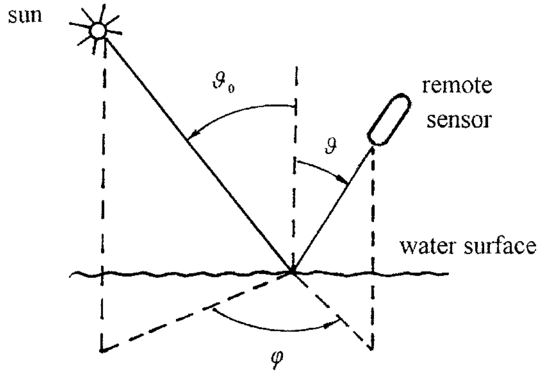

Figure 2. Sketch illustrating the notations of angles used in the numerical modelling. The altitude h and depth z are measured from the water surface and water body bottom respectively.

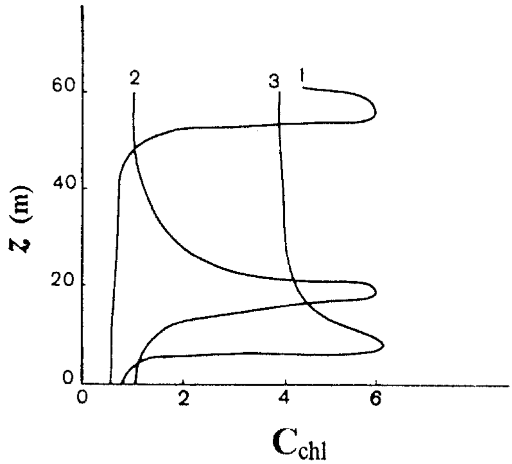

Figure 3. Vertical profiles (**1**–**3**) of C_{chl} (relative units) used in the Monte-Carlo simulations. The depth z is measured from the water body bottom.

viewing angle $\vartheta = 0°$, azimuth angle $\varphi = 0°$, altitude of observation $h = 1$ km, and zero wind speed) suggest the following conclusions. Variations in $L_u(\lambda)$ due to the chl vertical inhomogeneity do not exceed 10–15% (the error of our simulations is estimated at 5–10%) if C_{chl} undergoes substantial variations in the upper and middle layers of the water column. The presence or absence of the C_{chl} maximum in the lower layers affects $L_u(\lambda)$ even to a lesser extent. The effect of the C_{chl} profile shapes on $L_{rs}(\lambda)$ does not exceed several per cent points. In view of this result, and of all the uncertainties inevitably accompanying field measurements of hydro-optical parameters and characteristics of the radiation field, it appears only reasonable, at least for typical conditions occurring in Lakes Ladoga and Onega, to consider only the cases with homogeneous vertical profiles of chl, sm, and doc, when simulating the radiance field in the water body–atmosphere system.

Proceeding from the above finding, our further simulations aimed at studying angular and spectral variations of $L_u(\lambda)$ and were consequently run for vertically homogeneous distributions of principal OAC. Characteristics of the radiance field were computed letting the nadir and azimuthal viewing angles (ϑ, φ), the sun azimuth angle (ϑ_0), and wind speed above the water surface as well as the principal OAC concentrations vary within the realistic ranges inherent in the environments of Lake Ladoga.

According to Fisher and Grassl (1984), radiance $L_u(\lambda)$ emerging from beneath the water surface exhibits but a weak azimuthal dependence in case of clear oceanic waters. Our simulation experiments indicate that this quasi-isotropy is not characteristic of non-case I waters heavy-laden with chl, sm, and doc: $L_u(\lambda)$ proves to be maximal in the sun direction and highly dependent on the viewing angle ϑ unless $\vartheta < 30°$, and $\varphi > 90°$. Relevant experimental data obtained by us from *in situ* measurements (Kondratyev *et al.* 1990) confirm the above simulation results.

The spectral/angular behaviour of radiance $L_u(\lambda)$ in mesotrophic inland waters under calm weather conditions (i.e., the near surface wind speed $V = 0\ \mathrm{ms}^{-1}$), and varying ϑ_0, ϑ angles is shown in figure 4 for $\lambda = 410$, 500, 610, and 660 nm and $\varphi = 90°$. The graphs in figure 4 offer a clear evidence of a substantial decrease in

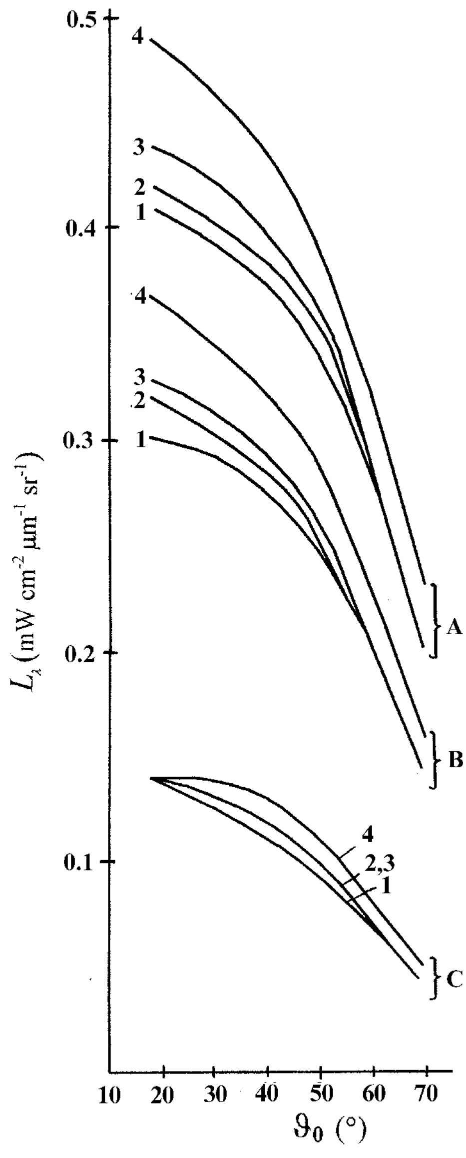

Figure 4. Variations of L_u against the sun zenith angle ϑ_0 for $\vartheta = 0°$ (**1**), 18° (**2**), 32° (**3**), 60° (**4**), and $\varphi = 90°$. **A**—$\lambda = 560$ nm; **B**—$\lambda = 500$ nm and $\lambda = 660$ nm (i.e., the two sets of curves (1–4) for both wavelengths practically coincide); **C**—$\lambda = 410$ nm. The water surface is assumed calm (i.e., $V = 0$ ms^{-1}). The OAC concentrations are taken equal to 5·6 μg l^{-1} (C_{chl}), 1 mg l^{-1} (C_{sm}), 8·5 mgC l^{-1} (C_{doc}). Altitude of observation $h = 1$ km.

$L_u(\lambda)$ in the short wavelength portion of the visible spectrum. This effect becomes even more pronounced at low values of ϑ_0, and slant viewing directions.

The ratio $P_\lambda = [L_u(\lambda)/L_{rs}(\lambda)] \times 100\%$ was chosen as a criterion of the information content inferable from remote sensing data provided by a sensor on a low-flying platform. Actually, this ratio is believed to account for the $L_u(\lambda)$ contribution to the net radiance signal $L_{rs}(\lambda)$ captured by a remote sensor. Figure 5 shows the variability of P_λ at $\lambda = 600$ nm for in-water conditions rather typical of Lake Ladoga. It could

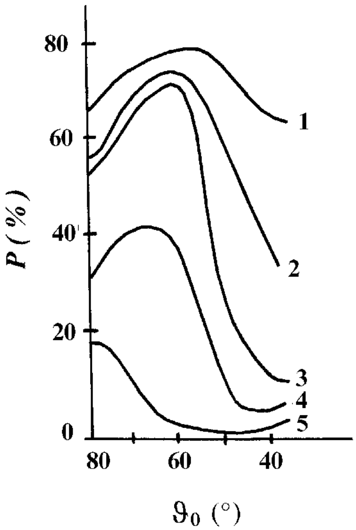

Figure 5. Dependence of P ($\lambda = 600$ nm) on ϑ_0 for $\vartheta = 0°$ (**1**), 10° (**2**), 20° (**3**), 40° (**4**), 60° (**5**) and $\varphi = 90°$. The water surface is assumed wind-roughened ($V = 5$ ms^{-1}). The OAC concentrations are taken equal to 10 μg l^{-1} (C_{chl}), 10 mg l^{-1} (C_{sm}), 7 mgC l^{-1} (C_{doc}). Altitude of observation $h = 1$ km.

be seen that the curves exhibit a distinct maximum whose height and position on the axis of solar zenith angles reveal a tendency to, respectively, decrease and shift to smaller ϑ_0 with increasing viewing angle ϑ. Figure 5 suggests that for nadir viewing, optimal conditions for remote sensing are attainable at $\vartheta_0 \approx 35°$.

The investigation of P_λ dependence on the azimuthal angle φ indicates that the maximum value of P_λ occurs at $\varphi \approx 90°$; and its height diminishes with decreasing ϑ (figure 6). As it could be seen from figure 6, the angular range where P_λ remains high and at the same time more or less isotropic extends well over $\varphi \approx 90°$. It appears essential in terms of routine remote sensing when it is practically impossible for several reasons to keep the current azimuth viewing angle at its strict optimal value.

Simulations of the wind effect impact on P_λ yielded results given in figure 7. An increase in the wind speed V inevitably entails a rapid drop of the P_λ value. With growing V, the optimal conditions of remote sensing could be reached at small viewing angles and high sun elevations.

The investigation of P_λ dependence on solar zenith angle for various wavelengths have shown that P_λ augments (provided $\vartheta < 50°$) with increasing ϑ_0 and λ. It might appear from figure 8 that large ϑ_0 are preferable for conducting remote sensing of natural water bodies. However, with the figure 4 data in mind, it could be stated that, the most favourable sun angles ϑ_0 should be about 35° when the radiance signal coming up from beneath the water surface is strong enough, and at the same its share in $L_{rs}(\lambda)$ remains still high.

4.2. *Water colour simulations*

Following the guidelines set out in section 2.2., and using digitized data on downwelling subsurface spectral irradiance measured *in situ* in Lake Ladoga in mid-summer time (Kondratyev *et al.* 1990), numerical simulations of water colour formation have been conducted in order to reveal the response of chromaticity

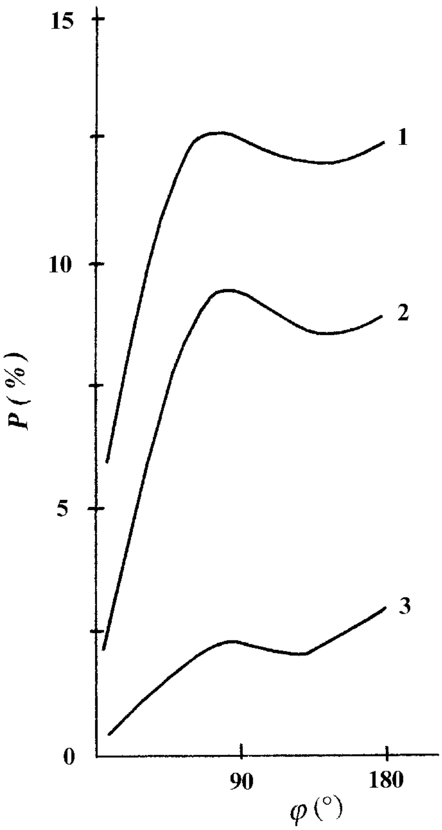

Figure 6. Dependence of P ($\lambda = 520$ nm) on φ for $\vartheta = 30°$ (**1**), 45° (**2**), 75° (**3**), at $\vartheta_0 = 30°$. The OAC concentrations are taken equal to 2 μg l^{-1} (C_{chl}), 0·5 mg l^{-1} (C_{sm}), 7 mgC l^{-1} (C_{doc}). Altitude of observation $h = 1$ km. The wind speed $V = 6$ ms^{-1}.

co-ordinates X, Y, Z, and the dominant wavelength λ_{dom} (as defined above, see equation (6) and figure 1 respectively) to variations in the principal OAC concentrations.

The analysis of the influence of the principal optically-active components on chromaticity coordinates suggests that their sensitivity to C_{chl} variations depend on the co-existing concentrations of C_{sm}, and C_{doc}: the higher C_{sm} and/or C_{doc}, the lesser the range of C_{chl} where the co-ordinates X, Y, and Z remain sensitive to C_{chl} variations (figure 9). This result fully agrees with the findings reported earlier by Jerome *et al.* (1994) for conditions appropriate for Canadian inland water bodies.

When analysing the dependence of λ_{dom} on the chl, sm, and doc concentration variations, it was found that simultaneously occurring low concentrations of sm and chl result in a short λ_{dom} ($\approx$473 nm) provided the doc concentration is also low. Interestingly, at $C_{doc} > 1$ mgC l^{-1} and the same minuscule concentrations of chl and sm, the dominant wavelength λ_{dom} attains a saturation value of about 478 nm, remaining invariable even if C_{doc} assumes abnormally high values ($\sim$1000·00 mgC l^{-1}). Nevertheless, this effect completely vanishes as soon as C_{sm} becomes 0·1 mg l^{-1} or more. A progressive growth of C_{chl} and C_{sm} at $C_{doc} < 1$ mgC l^{-1} result in a pronounced displacement of λ_{dom} to the longer wavelength region. This displacement of λ_{dom} proves to be particularly rapid when

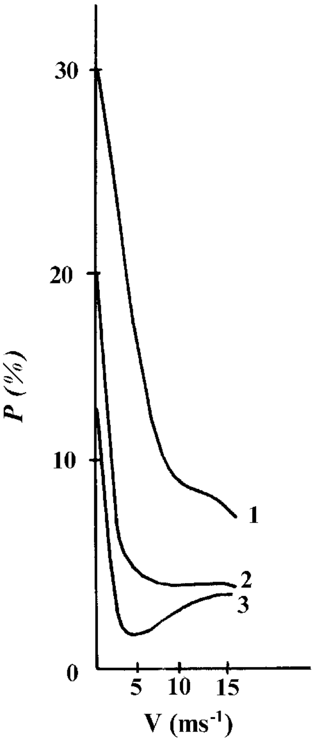

Figure 7. Dependence of P ($\lambda = 520$ nm) on wind speed (i.e., water surface roughness) **1**: $\vartheta_0 = 40°$, $\vartheta = 0°$; **2**: $\vartheta_0 = 40°$, $\vartheta = 30°$; **3**: $\vartheta_0 = 60°$, $\vartheta = 30°$. The OAC concentrations are taken equal to $2\ \mu g\ l^{-1}$ (C_{chl}), $0{\cdot}5\ mg\ l^{-1}$ (C_{sm}), $7\ mgC\ l^{-1}$ (C_{doc}). Altitude of observation $h = 1$ km. The azimuth viewing angle $\varphi = 90°$.

C_{doc} becomes $\geqslant 1{\cdot}2$–$2\ mgC\ l^{-1}$. At $C_{doc} \approx 8$–$10\ mgC\ l^{-1}$ λ_{dom} attains an end-point mounting up to about 575 nm (figure 10). This value of λ_{dom} compares well with the relevant colorimetric data retrieved from *in situ* measurements of the upwelling subsurface spectral radiance in Lake Ladoga as well as with the data reported for a number of rivers of British Columbia (Jerome *et al.* 1994). Figure 1 shows two-dimensional plots of Y and X locations of points M_1–M_2, representing water colour for hydrooptical conditions typical of the pelagic and coastal zone areas in Lake Ladoga (table 2). As it could be clearly seen, λ_{dom}, while varying but rather slightly over Lake Ladoga, remains close to a central value of about 570 nm. Although this result has been obtained for Lake Ladoga, the existence of an end-point for λ_{dom} is supposedly a fundamental property of natural water bodies heavily loaded with doc. According to Jerome *et al.* (1994), who used in their simulations the cross sections for Lake Ontario, λ_{dom} lies in the range 570–585 nm, provided $C_{chl} \geqslant 11\ \mu g\ l^{-1}$ or $C_{sm} \geqslant 5{\cdot}7\ mg\ l^{-1}$, at $C_{doc} > 6{\cdot}5\ mgC\ l^{-1}$.

Summarizing our simulation results it could be stated that (*a*) waters that contain simultaneously low concentrations of chl, sm, and doc appear blue to turquoise in colour; (*b*) highly turbid waters (i.e., waters containing high concentrations of sm and/or chl with low concentrations of doc display colours ranging from green to brown; and (*c*) waters with large concentrations of doc, irrespective of turbidity, provided that they possess some amounts of chl and sm, are invariably brownish. Furthermore, so far as the same colour may arise from a variety of OAC

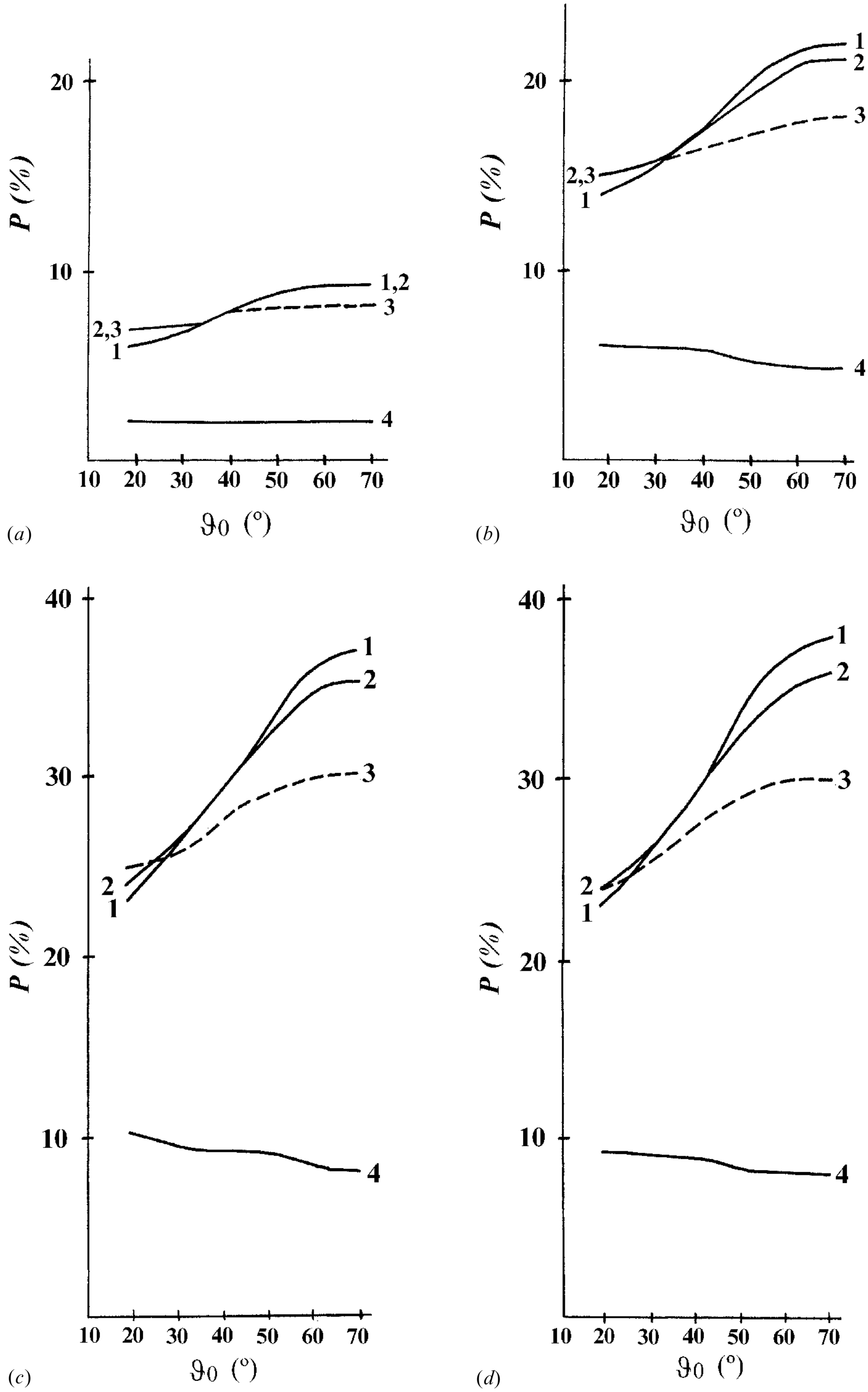

Figure 8. Angular variations P via ϑ_0 for $\lambda=(a)$ 410, (b) 550, (c) 560, (d) 660 nm, and $\varphi=90°$. **1**: $\vartheta=0°$, **2**: $\vartheta=18°$, **3**: $\vartheta=32°$, **4**: $\vartheta=60°$. The water surface is assumed calm (i.e., $V=0\ \mathrm{m\,s^{-1}}$). The OAC concentrations are taken equal to $5{\cdot}6\ \mu\mathrm{g\,l^{-1}}$ (C_{chl}), $1\ \mathrm{mg\,l^{-1}}$ (C_{sm}), $8{\cdot}5\ \mathrm{mgC\,l^{-1}}$ (C_{doc}). Altitude of observation $h=1$ km.

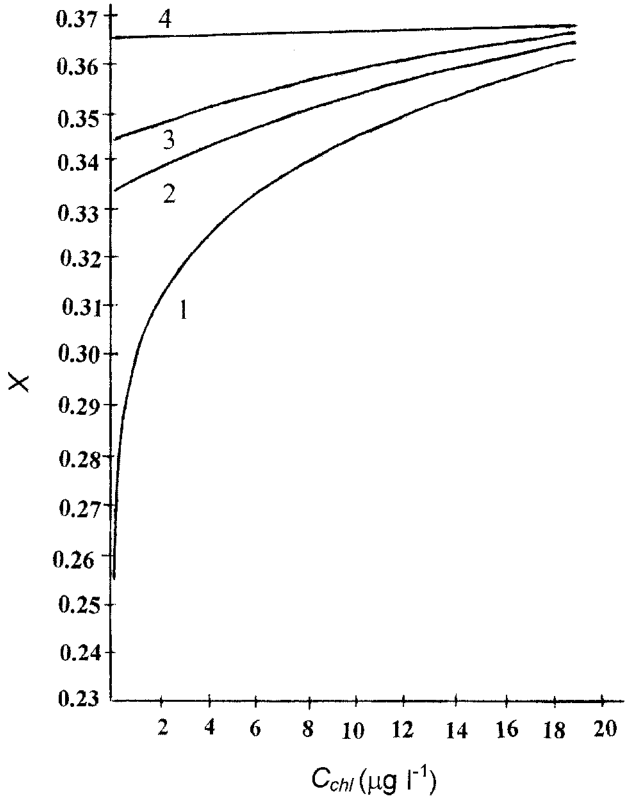

Figure 9. Sensitivity of the chromaticity coordinate X to variations in C_{chl} at various combinations of C_{sm} (mg l^{-1}) and C_{doc} (mgC l^{-1}): **1**: $C_{sm}=0$, $C_{doc}=2$; **2**: $C_{sm}=1$, $C_{doc}=2$; **3**: $C_{sm}=3$, $C_{doc}=2$; **4**: $C_{sm}=1$, $C_{doc}=8$.

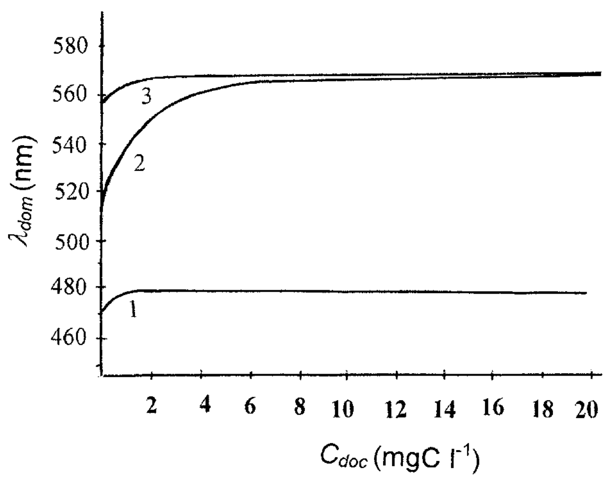

Figure 10. Sensitivity of λ_{dom} to variations in C_{doc} at three combinations of chl and sm concentrations (μg l^{-1}, and mg l^{-1}, respectively): **1**—$C_{chl}=C_{sm}\leqslant 0{\cdot}1$; **2**—$C_{chl}=2$, $C_{sm}=1$; **3**—$C_{chl}=10$, $C_{sm}=3$.

combinations, the purely colorimetric approach can hardly be used for quantitative or even qualitative assessments of aquatic environments status unless some *a priori* information is available on the probable abundance of doc or water turbidity. The larger the concentrations of OAC, the more futile would be attempts at separating the contributions of chl, sm, and doc to the λ_{dom} of the water colour. For case I waters that display a high degree of clarity, however, λ_{dom} may present a valuable means of determining C_{chl} and/or C_{doc}.

4.3. *Volume reflectance responsiveness to water quality status: implications for the retrieval algorithm development*

Model calculations of the volume reflectance conducted by Bukata *et al.* (1983) have revealed on a quantitative basis the spectral variations of the radiance coming out from beneath the water surface $L_u(\lambda)$ as a function of naturally occurring combinations of optically active components normally coexisting in natural waters. These simulations revealed two spectral regions centered at λ_i and λ_j, where $L_u(\lambda)$ appears to be, respectively, predominantly controlled by and almost insensitive to the presence of phytoplankton, provided the concentrations of suspended minerals (C_{sm}) and dissolved organic carbon (C_{doc}) are only marginal (i.e., a situation which is basically referred to as case I waters). Under these conditions, $L_u(\lambda)$ at $\lambda_i = 430$–450 nm decreases continuously (but not linearly) with the increasing phytoplankton concentration (the so called 'chlorophyll dip') due to the light absorption by chlorophyll molecules. At the same time the value of $L_u(\lambda)$ at $\lambda_j = 505$ nm (C_{sm}, and C_{doc} are nearly zero) or $\lambda_j = 570$–610 nm ($C_{doc} \cong 0$; $0{\cdot}1 < C_{sm} < 0{\cdot}5$ mg l^{-1}) remains invariable, i.e., $(\partial L_u/\partial C_{chl})_{\lambda=\lambda_j} = 0$. This finding obviously explains the feasibility of various regression relationships relating appropriate ratios of $L_u(\lambda)$ (or else values which could be derived from $L_u(\lambda)$) at two (sometimes, at several) wavelengths to a respective chl concentration in case I waters. Algorithmic expressions of this kind built up by numerous investigators for a wide variety of ocean and marine areas as well as lists of employed wavelengths (mostly adjusted to the CZCS sensor spectral bands) can be found in various reviews (see, for instance, Sathyendranath and Morel 1983, Kondratyev *et al.* 1990, Sturm 1993, McClain and Eyn 1994).

Nevertheless, as soon as the water column gets enriched in sm and/or doc (and consequently becomes non-case I water), the upwelling radiance $L_u(\lambda)$ undergoes some dramatic changes. First, the wavelength λ_j at which $(\partial L_u/\partial C_{chl})_{\lambda=\lambda_j} = 0$ no longer exists, and, second, the 'depth' of the chl dip can no more be related unambiguously to the chl loading as a result of the doc intervening adsorption in the shortwave portion of the visible spectrum. It means that for non case I waters the above parametric retrieval algorithms based on regressions relating C_{chl} (or the concentration of total suspended matter) to $L_u(\lambda)$ at two (or more) wavelengths could hardly be expected to provide precise retrievals and are strictly appropriate only to specific areas for which the statistics has been collected. The inappropriateness of applying case I waters chl-retrieval algorithms to non-case I, e.g., inland, waters is illustrated in figure 11. Therein chl concentrations determined for directly-collected water samples from Lake Ladoga are plotted against the chl concentrations inferred from simultaneously-obtained subsurface and above surface optical measurements. The data in figure 11 were obtained from 31 predominantly nearshore stations in a band around Lake Ladoga during the summer of 1989 (Kondratyev *et al.* 1990). The upwelling radiance spectra measured in the course of this field campaign, in

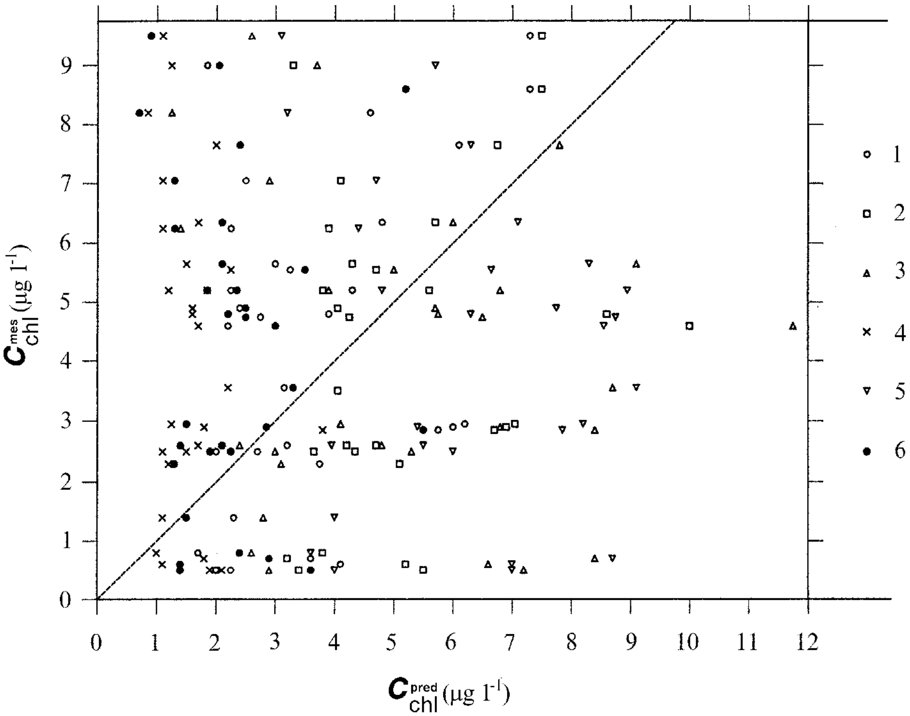

Figure 11. Directly-sampled chl concentrations in Lake Ladoga plotted against chl concentrations predicted by six different oceanic chl-retrieval algorithms taken from Gordon and Morel (1983).

$$\mathbf{1}\text{: } C_{\text{chl}}\ (\mu\text{g l}^{-1}) = 1\cdot69\left(\frac{L_u(520)}{L_u(550)}\right)^{-4\cdot45}; \qquad \mathbf{2}\text{: } 3\cdot326\left(\frac{L_u(520)}{L_u(550)}\right)^{-2\cdot439};$$

$$\mathbf{3}\text{: } 0\cdot78\left(\frac{L_u(443)}{L_u(550)}\right)^{-2\cdot12}; \qquad \mathbf{4}\text{: } 0\cdot50\left(\frac{L_u(443)}{L_u(550)}\right)^{-1\cdot27};$$

$$\mathbf{5}\text{: } 1\cdot62\left(\frac{L_u(460)}{L_u(560)}\right)^{-1\cdot40}; \qquad \mathbf{6}\text{: } 0\cdot55\left(\frac{L_u(443)}{L_u(520)}\right)^{-1\cdot81}.$$

conjunction with six different ocean/marine retrieval algorithms in widespread use (mathematical expressions are listed in figure 11 and have been taken from Gordon and Morel (1983)) were used to predict C_{chl}.

Nevertheless, regardless of the aforementioned objective physical reasons hampering the unconditional employment of regression algorithms of the type discussed so far, their attractiveness (first of all, due to their simplicity) stimulates further attempts to modify them so that they could be still applied to a wide range of natural water optical complexity. Gordon and Wang (1994) suggested an improved version of the retrieval algorithm for processing the forthcoming SeaWiFS data to be collected over the World Ocean. However, this new algorithm is based, as before, on the blue-green radiance ratio, and hence, susceptible to the limitations specified above. Tassan (1994) assuming the existence of a certain correlation between the concentrations of chl, sm and doc, suggested for the same sensor a locally applicable algorithm relating C_{chl} to X_c, where

$$X_c = [R(\lambda_2)/R(\lambda_5)][R(\lambda_1)/R(\lambda_3)]^{-1\cdot 2} \tag{8}$$

where R is the volume reflectance defined as the ratio of the subsurface upwelling to downwelling irradiances, and $\lambda_1, \lambda_2, \lambda_3, \lambda_5$ are the SeaWiFS spectral bands (412, 443, 490, and 555 nm, respectively). Analogous algorithms were generated by Tassan for retrieval of C_{sm} and C_{doc}. However, studies reviewed by Petrova (1995) indicate convincingly that in many inland and marine coastal waters the concentrations of major optically active components are basically not intercorrelated, while their spatial distributions are highly heterogeneous. No wonder that, for instance, a tentative application of the Tassan algorithms to Great Lakes failed to be satisfactory (Tanis and Pozdnyakov 1995). Obviously, a new generation of retrieval algorithms need to be developed to meet the fundamental requirement of being adjustable to varying hydrooptical situations.

Doerffer and Fisher (1994) suggested a two-flow radiative transfer approximation and a simplex optimization procedure to simultaneously infer aerosol path radiance and principal water quality parameters. Applied to the space imageries of the North Sea area, this optimization procedure proved to be efficient in providing spatial distributions of chl, sm and doc. The philosophy of this approach has much in common with the multivariate optimization and regularization techniques suggested, respectively by Levenberg (1944) and Marquardt (1963) and Tikhonov and Arsonin (1979), and much earlier (i.e., prior to the above publication of Doerffer and Fisher) successfully employed by Bukata *et al.* (1985) and Kondratyev *et al.* (1990).

The Levenberg-Marquardt (L-M) finite difference algorithm systematically determines for each wavelength of a measured subsurface irradiance reflectance spectrum $\{S_i\}$ a local minimum of $f(\boldsymbol{C})$ if a suitable initial value $\boldsymbol{C}_0$ is given (Bukata *et al.* 1985). Here

$$f(\boldsymbol{C}) = \sum g_i^2(\boldsymbol{C}) = \{[S_i - R(0, \boldsymbol{a}_i^*, \boldsymbol{b}_{b_i}^*, \boldsymbol{C})]/R(0, \boldsymbol{a}_i^*, \boldsymbol{b}_{b_i}^*, \boldsymbol{C})\}^2 \tag{9}$$

$\boldsymbol{C} = (1, C_{\mathrm{chl}}, C_{\mathrm{sm}}, C_{\mathrm{doc}})$, R is the volume reflectance computed through any pertinent parametrization (Gordon *et al.* 1975, Jerome *et al.* 1987), $\boldsymbol{a}^* = (a_w^*, a_{\mathrm{chl}}^*, a_{\mathrm{sm}}^*, a_{\mathrm{doc}}^*)$, $\boldsymbol{b}_b^* = (b_{b_w}^*, b_{b_{\mathrm{chl}}}^*, b_{b_{\mathrm{sm}}}^*)$ are the absorption and backscattering coefficient vectors respectively, a_j^*, $b_{b_j}^*$ ($j \equiv w$, chl, sm, doc) are, as above, absorption and backscattering cross sections of the principal OAC. The value of the concentration vector $\boldsymbol{C}$ for which $f(\boldsymbol{C})$ is the minimum will then be accepted as defining chl, sm, and doc abundances in the water column that produced the actually measured $\{S_i\}$.

This value of $f(\boldsymbol{C})$ may not, however, be the smallest achievable over the valid range of $\boldsymbol{C}$ since it might correspond not to the principal but to a local minimum of the analyzed function. Numerous starting concentration vectors $\boldsymbol{C}_{0_\xi}$ could be chosen to permit the L-M algorithm determining the corresponding minima $f_\xi(\boldsymbol{C})$. The $\boldsymbol{C}$ associated with the absolute minimum $f_\xi(\boldsymbol{C})$ of this set is then selected as the appropriate solution. Nevertheless, even pursuing this procedure there is no guarantee that any particular starting point $\boldsymbol{C}_{0_\xi}$ will result in the algorithm successfully finding any minimum for $f(\boldsymbol{C})$, since the algorithm may diverge. In addition, a $\boldsymbol{C}$ found through the minimization of $f(\boldsymbol{C})$, can prove to be physically meaningless (e.g., negative concentrations). To obviate such difficulties, constraints could be placed on $\boldsymbol{C}$ such that

$$C_{j_{\min}} \leqslant C_j \leqslant C_{j_{\max}} \tag{10}$$

where j refers to chl, sm, and doc. In addition, a transformation from the constrained $\boldsymbol{C}$ space to an unconstrained space could equally be effected using the classical error function relationship specified in (IMSL 1980).

The Tikhonov-Arsonin (T-A) approach as described by Kondratyev *et al.* (1990) assumes that the measured value of the volume reflectance

$$R_{\lambda} = A\boldsymbol{C}_j + \zeta_{\lambda} \tag{11}$$

where A is some operator, $\boldsymbol{C}_j$ is the concentration vector, ζ_{λ} is the error in R_{λ} measurements. It has been shown that the solution to the above equation could be found in the following way:

$$\Delta\boldsymbol{C} = (A^t\Sigma^{-1}A + D^{-1})^{-1}A^t\Sigma^{-1}\Delta R \tag{12}$$

where $\Delta R = R - R_0$, $\Delta\boldsymbol{C} = \boldsymbol{C} - \boldsymbol{C}_0$, $\boldsymbol{C}_0$ is some *a priori* given value of the concentration vector accounting for the optically active components which determine the value of R_{λ}; R_0 is the irradiance reflectance value at $\boldsymbol{C} = \boldsymbol{C}_0$; R is the actually measured value of the water column irradiance reflectance; D^{-1} is the R_{λ} dispersion matrix; Σ^{-1} is an *a priori* $\boldsymbol{C}_j$ dispersion matrix. Symbol t means that the matrix is a transposed one, whereas -1 stands for denoting an inverse matrix.

The solution for $\boldsymbol{C}$ can be found making use of the iteration procedure suggested by Timofeev *et al.* (1986):

$$\boldsymbol{C}_{j+1} = \boldsymbol{C}_0 + (A_j^t\Sigma^{-1}A_j + D^{-1})A_j^t\Sigma^{-1}(S(0,\lambda) - R_j(0,\lambda) + A_j(\boldsymbol{C}_j - \boldsymbol{C}_0)) \tag{13}$$

where according to the previously adopted notations, $\boldsymbol{C}_0$ is the initial value of the concentration vector $\boldsymbol{C}$; $\boldsymbol{C}_j$ is the value of vector $\boldsymbol{C}$ at an j-th iteration step computed with the application of the chosen R_{λ} parametrization; A_j is the variational derivatives $(\partial R/\partial C_j)$ matrix; Σ is the R_{λ} dispersion matrix; D is an *a priori* $\boldsymbol{C}_i$ dispersion matrix.

Consequently, this approach consists in minimization in the course of iteration of the standard deviation:

$$\sigma = n^{-1}\sum_{\lambda}[R^2(\lambda) - S^2(\lambda)] \tag{14}$$

which eventually plays the role of the vector $\boldsymbol{C}$ retrieval precision criterion.

The employment of both retrieval algorithms imply the availability of an adequate optical model appropriate for the chosen volume reflectance parametrization. The model described above for Lake Ladoga proves to be quite efficient in this respect. Indeed, applying both the L-M and T-A techniques to the measured R_{λ} in Lake Ladoga to infer the desired concentration vector $\boldsymbol{C}$, and comparing it with its directly (*in situ*) measured counterpart, we received good results. Figure 12 (*a*) shows a high degree of conformity between the retrieval (by means of the L-M technique) and validation results. Also, it is worthwhile comparing the two figures (11 and 12 (*a*)) which refer to the same lake and the same in-water conditions. The efficiency of the non-parametric retrieval algorithms in comparison with the parametric algorithms like those listed in figure 11 becomes quite evident from figure 12 (*a*). Apart from the precision considerations, the main asset of the non-parametric algorithms consists in a *simultaneous* retrieval of chl, sm, and doc concentrations (figures 12 (*a*), (*b*), and (*c*) from a *single* remote measurement of the entire visible radiance spectrum upwelling from a water body. Moreover, it should be emphasized that in case of optically complex waters a simultaneous retrieval of at least three principal co-existing OAC (chl, sm, and doc) is *indispensable* even if the actual goal of remote sounding is inferring the concentration of only *one* component, e.g., chl.

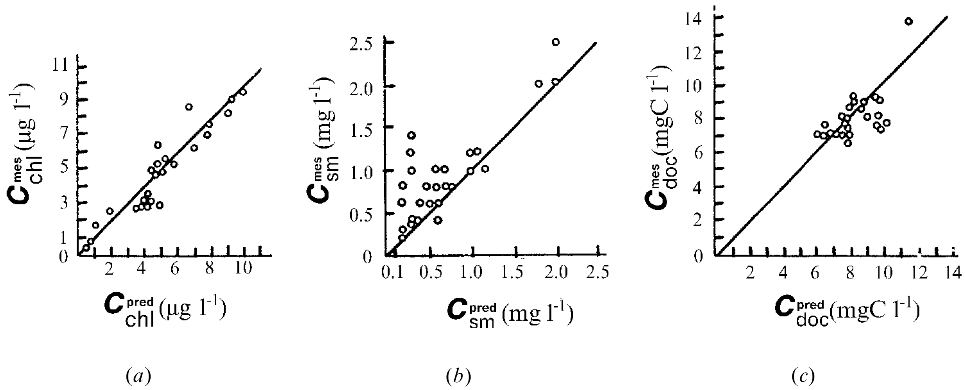

Figure 12. Directly-sampled chl, sm, and doc concentrations (C_{chl}^{mes}, C_{sm}^{mes}, C_{doc}^{mes}) in Lake Ladoga against chl (**a**). sm (**b**), and doc (**c**) concentrations predicted (C_{chl}^{pred}, C_{sm}^{pred}, C_{doc}^{pred}) through using the L-M multivariate optimization technique and the optical water quality model for Lake Ladoga.

5. Conclusion

The analyses conducted in this study strongly point to a necessity of developing non-regression approaches to the solution of the problem concerning optical remote sensing of natural water bodies laden with high, spatially variable, and mutually uncorrelated concentrations of principal OAC. Regression relationships relating the concentration of a sought for constituent to the ratio of water surface radiances at two or more wavelengths prove to be a reliable tool if applied to clear off-shore oceanic/marine waters (case I waters). Hydrooptically more complex waters of coastal zones as well as inland water bodies necessitate the application of non-parametric techniques capable of a more adaptable solution of the inverse problems.

The realization of such approaches implies the availability of hydrooptical models of basins liable to surveillance in form of tabulated spectral values of absorption and backscattering cross sections of principal OAC inherent in natural waters. Such models are already elaborated for North American and North European Great Lakes.

Investigation of the mechanisms of water colour formation for Lake Ladoga conditions has revealed a number of regularities which are believed to be equally applicable to a much larger selection of inland and marine coastal water masses (see Jerome *et al.* 1994). So far as the same colour may arise from a variety of OAC combinations, purely colorimetric approach can hardly be used for quantitative or even qualitative assessments of aquatic environments status unless some *a priori* information is available on the probable abundance of doc or water turbidity. The larger the concentrations of OAC, the more futile would be attempts at separating the contributions of chl, sm, and doc to the λ_{dom} of the water colour. For case I waters that display a high degree of clarity, however, λ_{dom} may present a valuable means of determining C_{chl} and/or C_{doc}.

The numerical Monte-Carlo simulations conducted by us for non-case I waters permitted to specify the optimal conditions for running remote sensing in the visible spectrum of natural water bodies from airborne platforms. The results obtained clearly indicate that both the spectral region and sun illumination as well as viewing geometries are of a paramount importance for a successful remote monitoring. Since these parameters are dependent on the composition of natural waters, it is mandatory that the performance of airborne monitoring be invariably preceded by a thorough analysis of the actual hydro-optical situation in the water body to be surveyed.

References

Austin, R. W., 1974, The remote sensing of spectral radiance from below the ocean surface. In *Optical aspects of oceanography*, edited by T. Platt (Oxford: Elsevier), pp. 317–344.

Bukata, R. P., Bruton, J. E., and Jerome, J. H., 1981, Optical water quality model of Lake Ontario: 2. Determination of chlorophyll-a and suspended mineral concentrations of natural waters from submersible and low altitude optical sensors. *Applied Optics*, **20,** 1704–1714.

Bukata, R. P., Bruton, J. E., and Jerome, J. H., 1983, Use of chromaticity in remote measurements of water quality. *Remote Sensing of Environment*, **3,** 161–177.

Bukata, R. P., Bruton, J. E., and Jerome, J. H., 1985, *Application of Direct Measurements of Optical Parameters to the Estimation of Lake Water Quality Indicators* (Burlington, Ontario: National Water Research Institute (NWRI)).

Bukata, R. P., Jerome, J. H., Kondratyev, K. Ya., and Pozdnyakov, D. V., 1991, Estimation of organic and inorganic matter in inland waters: optical cross sections of Lakes Ladoga and Ontario. *Journal of Great Lakes Research*, **17,** 461–469.

Bukata, R. P., Jerome, J. H., Kondratyev, K. Ya., and Pozdnyakov, D. V., 1995, *Optical Properties and Remote Sensing of Inland and Coastal Waters* (Boca Raton: CRC Press).

Clarke, G. L., Ewing, G. C., and Lorenzen, C. J., 1970, Spectra of backscattered light from the sea obtained from aircraft as a measure of chlorophyll concentrations. *Science*, **167,** 1119–1121.

Commité International de L'Eclairage (CIE), 1957, *Vocabulaire Internationale de l'Eclairage* (Paris: CIE).

Dekker, A. G., Malthus, T. J., and Hoogenboom, 1995, The remote sensing of inland water quality, In *Advances in Remote Sensing*, edited by F. M. Danson and S. E. Plummer (Chichester: John Wiley), pp. 123–142.

Doerffer, R., and Fisher, J., 1994, Concentrations of chlorophyll, suspended matter, and gelbstoff in case II waters derived from satellite coastal zone colour scanner data with inverse modelling methods. *Journal of Geophysical Research*, **99,** 7457–7466.

Dubovik, O. V., Ostchepkov, C. L., and Lapionok, T. V., 1994, An integration-regularization method of non-linear inverse problems solution and its applciation for the interpretation of the radiance spectra of water surface, Izvestia AN. *Fizika Atmosphery I Okeana* [Proceedings of the Russian Academy of Sciences, Physics of the Atmosphere and Ocean], **30,** 106–113.

Fadeev, V. V., and Churbanov, V. V., 1981, Quantitative determination of oil products in water via laser spectroscopy methods. *Doklady Akademii Nauk SSSR* [Proceedings of the USSR Academy of Sciences], **261,** 342–346.

Fisher, J., and Grassl, H., 1984, Radiative transfer in an atmosphere-ocean system: an azimuthally dependent matrix-operator approach. *Applied Optics*, **23,** 1032–1039.

Fisher, J., Doerffer, R., and Grassl, H., 1991, Remote sensing of water substances in rivers, estuarine and coastal waters. In *Biogeochemistry of Major World Rivers*, edited by E. T. Degens and J. E. Richey (Chichester: John Wiley), 25–55.

Gordon, H. R., and Morel, A. Y., 1983, *Remote Assessment of Ocean Colour for Interpretation of Satellite Visible Imagery* (Berlin: Springer-Verlag).

Gordon, H. R., and Wang, M., 1994, Retrieval of water-leaving radiance and aerosol optical thickness over the oceans with SeaWiFS: a preliminary algorithm, *Applied Optics*, **33,** 443–452.

Gordon, H. R., Brown, O. B., and Jacobs, M. M., 1975, Computed relationships between the inherent and apparent optical properties of a flat homogeneous ocean. *Applied Optics*, **14,** 417–427.

Guitelson, A. A., Nikanorov, A. M., Szabo, Gy., and Szilagyi, F., 1986, Étude de la qualité des eaux de surface par télédétection. In *Monitoring to Detect Changes in Water Quality Series. Proceedings of the Budapest Symposium, July 1986*, IAHS Publ. 157 (Budapest: IAHS), pp. 111–121.

Henderson-Sellers, B., and Markland, H. R., 1987, *Decaying Lakes* (Chichester: John Wiley).

Hooker, S. B., and Esaias, W. E., 1993, An overview of the SeaWiFS Project. *EOS Transactions*, **74,** 241–246.

International Mathematical and Statistical Library (IMSL), 1980, *The IMSL Reference Manual* (Houston: IMSL, Inc).

Jerome, J. H., Bukata, R. P., and Bruton, J. E., 1987, Monte Carlo determinations of volume reflectance for natural waters. National Water Research Institute (NWRI) Publ. No. 67-149, Burlington, Ontario, Canada.

Jerome, J. H., Bukata, R. P., Whitefield, P. H., and Rousseau, N., 1994, Colours of natural waters. I. Factors controlling the dominant wavelength. *Northwest Science*, **68,** 43–52.

Kargin, B. A., 1983, *On a Statistical Modelling of Optical Radiation Interaction with a Wind-Roughened Sea Surface* (Novosibirsk: Nauka).

Kirk, J. T. O., 1983, *Light and Photosynthesis in Acquatic Ecosystems* (Cambridge: Cambridge University Press).

Kirk, J. T. O., 1984, Dependence on relationship between inherent and apparent optical properties of water on solar altitude. *Limnology and Oceanography*, **29**, 357–374.

Kondratyev, K. Ya., 1992, *Global Climate* (St Petersburg: Nauka).

Kondratyev, K. Ya., and Pozdnyakov, D. V., 1985, *Approaches to Remote Monitoring of Natural Water Quality* (Leningrad: Nauka).

Kondratyev, K. Ya., Kanter, R. R., Kargin, B. A., and Pozdnyakov, D. V., 1987, *Numerical Simulations in the Problems of Optical Remote Sensing of Inland Waters* (Leningrad: Nauka).

Kondratyev, K. Ya., Pozdnyakov, D. V., and Isakov, V. Yu., 1990, *Radiation and Hydro-optical Experiments in Lakes* (Leningrad: Nauka).

Levenberg, K. A., 1944, Method for the solution of certain nonlinear problems in least squares. *Quarterly Journal of Applied Mathematics*, **11,** 164–168.

Marquardt, D. W., 1963, An algorithm for least-squares estimation of non-linear parameters. *Journal of International Society of Applied Mathematics*, **2,** 164–168.

McClain, C. R., and Eyn, E.-N., 1994, CZCS bio-optical algorithm comparison. In *SeaWiFS Technical Report Series*, edited by S. B. Hooker, and E. R. Firestone (Washington, DC: NASA), pp. 3–52.

McClatchey, R. A., Bolle, H.-J., and Kondratyev, K. Ya., 1982, Cloudless standard atmosphere for radiation computation. Report of the International Association for Meteorology and Atmospheric Physics (IAMAP) on a Standard Radiation Atmosphere, Word Meteorological Ogranization/IAMAP, Boulder, Colorado.

Melack, J. M., 1983, Large, deep salt lakes: a comparative limnological analysis. *Hydrobiologia*, **105,** p. 223–230.

Morel, A., and Prieur, L., 1977, Analysis of variations in ocean colour. *Limnology and Oceanography*, **22,** 709–722.

NASA, 1986, Coastal zone imagery for selected coastal regions. Level II: Photographic Product. Park Ridge Il.: The Water. NASA Publication/A. Bohan Co., Washington, DC.

Petrova, N. A., 1995, *Phytoplankton successions and eutrophication of large lakes* (St Petersburg: Nauka).

Sathyendranath, S., and Morel, A., 1983, Light emerging from the sea—interpretation and uses in remote sensing. In *Remote Sensing Applications in Marine Science and Technology*, edited by A. P. Cracknell (Dordrecht: Reidel), pp. 323–357.

Schiller, H., and Doerffer, R., Neural network for emulation of an inverse model-operational derivation of case II water properties. In *Proceedings of the Fourth International Conference on Remote Sensing for Marine and Coastal Environments, Orlando, Florida, 17–19 March 1997*, Volume II (Ann Arbor: ERIM Publ.), p. 1.

Sturm, B., 1993, CZCS data processing algorithms. In *Ocean Colour: Theory and Application in a Decade of CZCS Experience*, edited by V. Barale and P. M. Shlittenhardt (Brussels and Luxembourg: ECSC, EEC, EAEC), pp. 95–116.

Tanis, F. J., and Pozdnyakov, D. V., 1995, Evaluation of proposed coastal ocean colour algorithms for retrieval of bio-pigments and suspended sediments in the Great Lakes. In *Proceedings of the Third Thematic Conference on Remote Sensing for Marine and Coastal Environments* (Ann Arbor: ERIM), pp. I/140–I/150.

TASSAN, S., 1994, Local algorithms using SeaWiFS data for the retrieval of phytoplankton pigments, suspended sediment, and yellow substance in coastal waters. *Applied Optics*, **33,** 2369–2378.

TIKHONOV, A. N., and ARSONIN, V. YA., 1979. *Methods of Incorrect Problem Solution* (Leningrad: Nauka).

TIMOFEEV, YU. M., and ROSANOV, V. V., 1986, A multispectral method of determining vertical profiles of O_3, O_2 and aerosol attenuation in the atmosphere. *Meteorology and Hydrology,* **8,** 66–73.

YERLOV, N. G., 1976, *Marine Optics* (Amsterdam: Elsevier).